Journal of Radiation Researches, vol.10, No.2, 2023, Baku
Investigation of raw ceramic paste as a matrix for the solidification of radioactive waste
pp. 36-43

PACS: 78.60.Kn

INVESTIGATION OF RAW CERAMIC PASTE AS A MATRIX FOR THE SOLIDIFICATION OF RADIOACTIVE WASTE

S.G. Mammadov, M.A. Gurbanov, A.Z. Abishov, A.S. Ahadova, A.B. Ahadov

Institute of Radiation Problems, MSE AR
s.mammadov@irp.science.az

Abstract: The paper presents thermogravimetric (TG), thermoluminescence (TL), and X-ray diffraction (XRD) studies on a raw ceramic paste that can be used as an alternative for cement in mortar recipes prepared with recycled radioactive concrete for the solidification of radioactive waste. The results of TG and differential thermal analysis (DTG) indicate that the primary mass loss of 8 to 15 wt.% in the sample can be attributed to the evaporation of adhesion water at temperatures below 350°C, as well as the dehydration of structural water at higher temperature ranges. XRD patterns of raw ceramic paste indicate the presence of clay minerals like montmorillonite and muscovite, quartz, and felspars. The dehydroxylation process of montmorillonite is characterized by distinct peaks in the DTA curves, providing insights into the structural changes taking place. The TL properties of quartz, including TL emission and dose-response, are explored, allowing for the estimation of the saturation dose at 13.2 kGy.

Keywords: montmorillonite, calcite, clay, thermogravimetry, thermoluminescence, radioactive waste.

1. Introduction

Radioactive waste is generated across a range of applications involving the use of radionuclides, encompassing nuclear power plants and medical industries [1][2]. The primary objective in managing these waste products is to safely isolate radioactive contamination from the natural environment. To achieve this, inert materials are typically employed to impede the movement of radionuclides during extended periods of storage and disposal [2–4], thereby minimizing the risk of environmental contamination.

One established method for encapsulating low- and intermediate-level radioactive waste is through cementation, a process that has been employed for numerous years due to its cost-effectiveness and the ready availability of cement-based materials [4–6]. However, an inherent limitation of many cement-based materials is their susceptibility to erosion when exposed to groundwater [7] which heightens the potential for leaching of radioactive contaminants from the waste matrix.

In essence, the challenge in managing radioactive waste lies in developing materials and containment strategies that ensure long-term isolation of the radioactive substances from the environment while withstanding the erosive effects of groundwater and maintaining thermal stability.

Hence, there is a concerted effort underway to advance the development of materials that can effectively immobilize radionuclides. These materials include sulfoaluminate cement, composites of cement and natural clay, aluminum cement, glasses, ceramics, and geopolymers [8–10].

The smectites and kaolinites comprise the main part of row ceramic paste and are widely used for the manufacturing of ceramics for a wide range of purposes including nuclear waste management and simple domestic goods. The decommissioning of nuclear facilities produces a

large amount of radioactive waste and most of them are concrete waste [11]. The volume reduction and recycling of waste are essential to reduce waste management costs by using ceramic pastes.

Ceramic-based materials are increasingly recognized as a crucial component within the engineered barrier system designed for the extended disposal of radioactive waste. Consequently, it is imperative to understand the impact of ionizing radiation on these materials to instill confidence in their long-term stability.

In this paper, the thermogravimetric, XRD, and TL properties of a raw ceramic paste are investigated in response to irradiation and heat treatment as an alternative for cement in the mortar recipes prepared with recycled radioactive concrete to solidify radioactive waste.

2. Materials and methods

The PXRD analysis of the samples was performed using a D2Phaser (Bruker) diffractometer with Ni-filtered CuKα radiation (λ=1.5406 A), and the samples were randomly oriented. Scans were conducted within the $5 \leq 2\Theta \leq 75°$ range at a scanning speed of 1.2°/min. Semiquantitative measures were obtained from the PXRD data to estimate the abundance of mineral phases, including specific reflection intensities, density, and mass absorption coefficients for CuKα radiation. Mineral phase identification was accomplished using the DIFFRAC.SUITE software, employing the TOPAS non-standard quantitative phase and structure analysis program, along with ICDD powder databases. The Reference Intensity Ratio (RIR) method, which utilizes established in-house RIR values, was employed for semiquantitative approximations of mineral phase abundances. This method is universally applicable for quantitative phase analysis in X-ray powder diffraction [14]. To determine the proportion of amorphous material, the area of the broad background hump representing amorphous material in each sample was compared to the corresponding area of standard mixtures containing varying concentrations of natural amorphous material. These standard mixtures were subjected to scanning under identical conditions. A semiquantitative estimation of the percentage of total amorphous material was subsequently obtained.

For thermogravimetric and differential thermal analysis of ceramic powders, a Perkin Elmer STA6000 Simultaneous Thermal Analyzer was utilized. The analysis involved heating the samples from ambient to 950°C at a heating rate of 5°C. The balance sensitivity was set at 0.1μg, and a nitrogen gas flow of 20 ml/min was maintained.

The irradiation was performed at an ambient temperature from a ^{60}Co source at different dose levels ranging up to 3.5 kGy. A dose rate of the ^{60}Co source has been determined by Magnettech Miniscope MS400 EPR Spectrometer using individually wrapped, barcode-labeled BioMax Alanine Dosimeter Films (developed by Eastman Kodak Company). The irradiated samples were weighed to 5±0.5 mg and read out after one day in an N_2 atmosphere in a Harshaw 3500 manual reader using the linear heating rate of 5ºC/s.

Luminescence measurements were performed to find out the dose-response of the ceramic paste. The samples were crushed into powder and sieved into three-size fractions. The 90÷150 mm fraction was then etched in HF and washed in HCl [12]. The measurement sample comprised quartz inclusions with a size greater than 90 mm and a density between 2.63 and 2.67 g/cm3, separated using sodium poly tungstate [13,14]. As a result of the development of the methodology, it was found that the best measurement results are obtained when using powder samples, thus achieving more uniform heating; the weight of the sample is about 5 mg, and the particle size is 0.1-0.25 mm.

3. Results and discussions

Fig. 1 illustrates the outcomes of TG/DTG/DTA experiments performed on a raw ceramic paste sample, indicating two distinct stages of mass loss and the absence of calcite in the investigated material. The raw ceramic pastes (CP1 and CP2) serve as contemporary examples created by a skilled potter near the archaeological site, utilizing locally sourced raw materials. The DTG curve, representing the derivative of mass loss (dm/dt), provides a clearer delineation of the mass loss steps. The mass loss percentages for both samples are as follows: dehydration represents 8.06% (CP1) and 15.0% (CP2) of the total mass loss, whereas the decomposition of hydroxyls accounts for 3.16% (CP1) and 5.45% (CP2) of the total mass loss.

In general, raw ceramic paste comprises clay minerals (such as smectites and kaolinites) and tempering materials like quartz, feldspar, calcite, and organic fillers. During mild firing (where the temperature is ≤700°C), changes are primarily observed in the clay component, as the tempering materials exhibit higher thermal stability [15]. It is commonly accepted that mass loss during clay heating can be attributed to three stages: (I) dehydration (≤350°C), (II) decomposition of hydroxyls (350–600°C), and (III) decomposition of carbonates, particularly calcite (600–850°C), if present in the source material [15,16]. Additional transformations occur at higher temperatures. Beyond 1000°C, the ceramic paste undergoes a transition into a glassy substance containing dispersed particles of the added tempering materials. This transformation is irreversible, and the resulting product bears little resemblance to the original ceramic paste. However, it is important to note that this confirmation holds true primarily when montmorillonite predominates as the clay material, as it encompasses both bound water and hydroxyl groups within its composition. In contrast, dehydroxylation causes kaolinite to begin losing mass at temperatures around 400°C and above [17]. The extent of mass loss following dehydroxylation varies depending on the specific clay mineral. During the firing of montmorillonite and kaolinite, clay minerals undergo transformation into an anhydrous amorphous phase. It is important to note that the processes being discussed are highly intricate, and the temperature intervals mentioned are conditional.

Fig. 1 illustrates the phenomenon of dehydration, which is characterized by a complex endothermic peak in the temperature range below 350°C and a corresponding mass loss of up to 15%. The shape of the dehydration peak can vary depending on several factors, potentially resulting in double or triple peaks.

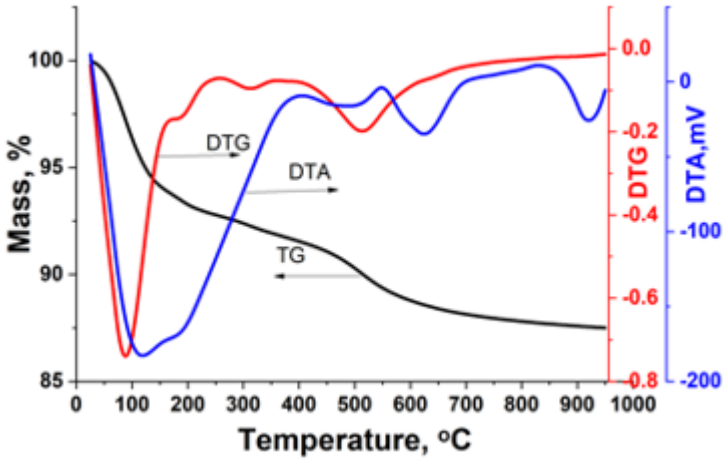

Fig. 1. TG, DTG and DTA profiles of raw ceramic paste

The quantity of water adsorbed on montmorillonite is notably influenced by the relative humidity of the external atmosphere, the type of cations occupying the exchangeable sites within the layered structure, the grain diameter distribution of the sample, and the concentration of structural defects. Previous studies have demonstrated that the dehydration peak appears as a single peak when the exchangeable sites are occupied by cations with a charge of +1. However, in the presence of alkaline earth and other cations with a charge of +2, the peak is observed to be doubled [18].

The occurrence of a complex-shaped endo-exotherm in the temperature range of 900-1000°C signifies the emergence of novel phases, including spinel, cristobalite, and mullite [19].

The investigation of montmorillonite rehydration in hydrothermal conditions is significant as it sheds light on the alterations that clay minerals undergo naturally, particularly in relation to the preservation of radioactive waste materials. It has been observed that the threshold for reversible hydration is around 600°C. When montmorillonites are heated to temperatures above 500-600°C under atmospheric conditions, the subsequent rehydration process is only partial and occurs at a very slow rate, often taking hundreds of days [18].

The DTA curves (Fig. 1) clearly exhibit the dehydroxylation process of montmorillonite, manifested by two distinct peaks. The first peak occurs around 500°C, while the second peak occurs at approximately 700°C.

Various possible factors have been proposed to explain this two-stage dehydroxylation phenomenon. These include substitution occurring in the tetrahedral and octahedral layers, with the involvement of elements like iron, as well as structural defects within the montmorillonite matrix (as discussed in references [18]).

XRD patterns of raw ceramic paste indicate the presence of clay minerals like montmorillonite (PDF 00-060-0318) and muscovite (PDF 01-072—0496), quartz (PDF 01-070-7344), and felspars (albite- PDF 00-041-1480) as a tempering material (Fig. 2). Fig. 2 shows that both samples of raw ceramic paste do not contain calcite in their composition.

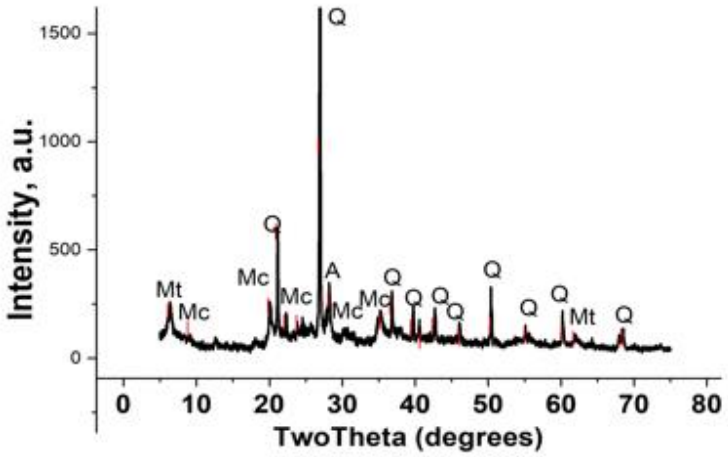

Fig. 2. XRD patterns of raw ceramic paste (sample CP1)
Mt-montmorillonite; Mc-muscovite; Q-quartz; A-albite (feldspar)

Thermoluminescence (TL) emission of light can be characterized as a form of delayed phosphorescence, which occurs due to the accumulation of metastable electrons and holes in defects within materials such as quartz or other crystalline insulators. This accumulation is a result of ionizing radiation, and the subsequent recombination of these electrons and holes takes place

upon heating, facilitated by phonons. The intensity of TL signals varies with the absorbed dose, under specific conditions such as dose rate and material, and can be represented by a dose-response curve.

Irradiated quartz grains exhibit several TL peaks when heated from room temperature to 450°C [20]. It has demonstrated that the peak height could be used to monitor dose-dependent sensitivity changes observed after heating to 500°C. Fig. 3 illustrates the dose dependence of the TL glow curve. Samples were irradiated with a ^{60}Co gamma source then TL glow-curves were measured after two days.

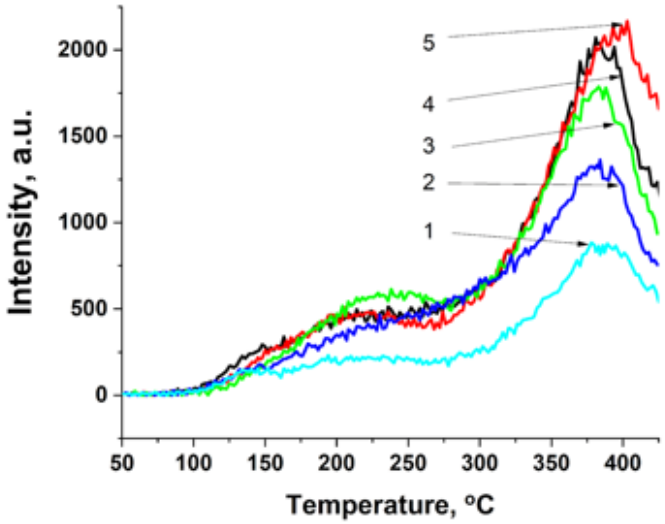

Fig. 3. Dose dependence of TL intensity irradiated quartz extracted from the ceramic paste and irradiated at (1) 1.4 kGy; (2) 1.9 kGy; (3) 2.44Gy: (4) 2.8 kGy; (6) 3.3 kGy

Dose-response curves can take different forms, including linear, superlinear, sublinear, and supralinear forms [21]. In TL dating, the choice of a mathematical function for fitting the dose-response data points should meet two essential criteria: it should have a physical basis and accurately fit the experimental data points. In practice, polynomial or linear approximations are often used for low doses, while saturating exponential fits are employed for moderate doses. The application of a single saturating exponential (SSE) function assumes that the TL signal is generated by a single electron trap. The dependence of the TL signal intensity (in arb. units) in quartz extracted from the ceramic mass on the adsorbed dose is shown in Fig. 4.

As depicted in Fig. 4, the TL intensity demonstrates a dose-dependent increase until it reaches a saturation point after a certain dose threshold. This behavior is typically attributed to the competition between transitions into trapping states or recombination centers, which occur during irradiation excitation, sample heating, or both. At higher excitation doses, it is generally observed that the dose dependence function becomes sublinear as it approaches saturation. This is commonly explained by the filling of trapping states and/or recombination centers to their maximum capacity, resulting in no additional increase in emitted TL with further irradiation. The applied SSE fitting function allows to estimation the saturation dose for the test sample, which is defined as 13.2 kGy.

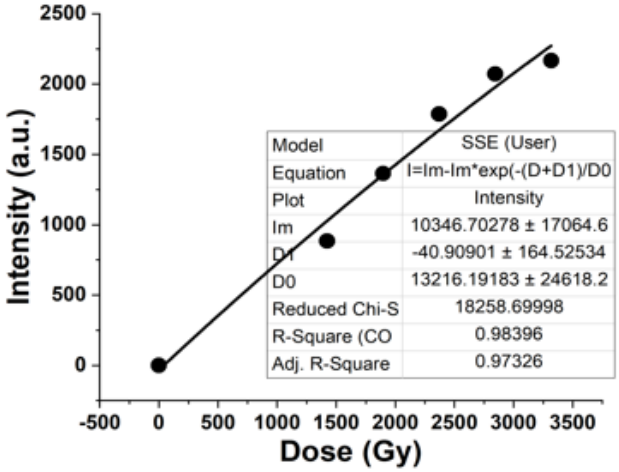

Fig. 4. Dependence of the intensity of the TL signal (in arbitrary units) in quartz extracted from ceramic paste on the adsorbed dose

4. Conclusions

The complex characterization of ceramic paste, which includes a description of its mineralogical, chemical, and thermal properties, was provided in an interdisciplinary approach using thermogravimetric (TG), thermoluminescence (TL), and X-ray diffraction (XRD). The experimental findings shed light on various aspects of the raw ceramic paste sample, including its thermal behavior, composition, and transformation during the firing process.

XRD analysis of ceramic paste reveals that investigated samples contain minerals like quartz, feldspar, and montmorillonite.

The dehydroxylation process of montmorillonite is characterized by distinct peaks in the DTA curves, providing insights into the structural changes taking place. The TL properties of quartz, including TL emission and dose-response, are explored, allowing for the estimation of the saturation dose at 13.2 kGy.

These findings contribute to our understanding of the material's properties and behavior, with implications in various fields. The investigation of rehydration in montmorillonite under hydrothermal conditions offers insights into natural clay mineral alterations, which are particularly relevant to the preservation of radioactive waste. Furthermore, the analysis of TL properties in quartz opens avenues for applications in radioactive waste management, as TL can serve as a dosimetric tool to estimate absorbed radiation doses.

References

1. N. Yamaguchi, S. Eguchi, H. Fujiwara, K. Hayashi, H. Tsukada, Sci. Total Environ. 425 (2012) 128–134.
2. Q.-H. Hu, J.-Q. Weng, J.-S. Wang, J. Environ. Radioact. 101 (2010) 426–437.
3. W.E. Lee, M.I. Ojovan, M.C. Stennett, N.C. Hyatt, Adv. Appl. Ceram. 105 (2006) 3–12.
4. M.I. Ojovan, G.A. Varlackova, Z.I. Golubeva, O.N. Burlaka, J. Hazard. Mater. 187 (2011) 296–302.
5. Z. Xu, Z. Jiang, D. Wu, X. Peng, Y. Xu, N. Li, Y. Qi, P. Li, Ceram. Int. 43 (2017) 4434–4439.

6. A.M. El-Kamash, M.R. El-Naggar, M.I. El-Dessouky, J. Hazard. Mater. 136 (2006) 310–316.
7. R.O. Abdel Rahman, A.A. Zaki, A.M. El-Kamash, J. Hazard. Mater. 145 (2007) 372–380.
8. Q. Li, Z. Sun, D. Tao, Y. Xu, P. Li, H. Cui, J. Zhai, J. Hazard. Mater. 262 (2013) 325–331.
9. Z. Zhang, C. Zhao, Y. Rao, C. Yu, Z. Luo, H. Zhao, X. Wang, C. Wu, Q. Wang, Sci. Total Environ. 892 (2023).
10. L. Junfeng, L. Chen, J. Wang, Prog. Nucl. Energy 141 (2021) 103957.
11. W.K. Choi, B.Y. Min, K.W. Lee, in: Vol. 5 Fuel Cycle High Low Lev. Waste Manag. Decommissioning; Comput. Fluid Dyn. (CFD), Neutronics Methods Coupled Codes; Instrum. Control, ASMEDC, 2009, pp. 193–196.
12. I. Bailiff, N. Holland, Radiat. Meas. 32 (2000) 615–619.
13. A.K. Singh, I. Manna, P.P. Kumar, A. Dawar, P.P. Kumar, M.K. Murari, Quat. Geochronol. 72 (2022) 101315.
14. S. Woor, J.A. Durcan, S.L. Burrough, A. Parton, D.S.G. Thomas, Quat. Geochronol. 72 (2022) 101368.
15. V. Molodin, L. Mylinkova, N. Shtertser, I. Durakov, V.A. Drebushchak, Chem. Sustain. Dev. 27 (2019) 101–108.
16. V.A. Drebushchak, L.N. Mylnikova, T.N. Drebushchak, J. Therm. Anal. Calorim. 133 (2018) 135–176.
17. R. Deju, A. Cucos, M. Mincu, C. Tuca, Rom. J. Phys. 66 (2021).
18. V.Š. Fajnor, K. Jesenák, J. Therm. Anal. 46 (1996) 489–493.
19. C.B. Hedley, G. Yuan, B.K.G. Theng, Appl. Clay Sci. 35 (2007) 180–188.
20. M.J. Aitken, Thermoluminescence Dating, Academic Press INC., 1985.
21. J.L. Lawless, R. Chen, D. Lo, V. Pagonis, J. Phys. Condens. Matter 17 (2005) 737–753.
22. G.L. Bykov, A. V Gordeev, T.K. Yurik, B.G. Ershov, High Energy Chem. 42 (2008) 211–214.
23. G.L. Bykov, E.V. Abkhalimov, V.A. Ershov, B.G. Ershov, Constr. Build. Mater. 295 (2021) 123644.
24. G.L. Bykov, V.A. Ershov, B.G. Ershov, Constr. Build. Mater. 252 (2020).

ИССЛЕДОВАНИЕ СЫРОЙ КЕРАМИЧЕСКОЙ ПАСТЫ КАК МАТРИЦЫ ДЛЯ ЗАТВЕРДЕНИЯ РАДИОАКТИВНЫХ ОТХОДОВ

С.Г. Мамедов, М.А. Гурбанов, А.З. Абишов, А.С. Ахадова, А.Б. Ахадов

Резюме: В статье представлены термогравиметрические (ТГ), термолюминесцентные (ТЛ) и рентгеновские дифракционные (РФА) исследования сырой керамической пасты, которая может быть использована в качестве альтернативы рецептурам цемента в строительных растворах, приготовленных из переработанного радиоактивного бетона для затвердевания радиоактивных отходов. Результаты ТГ и дифференциально-термического анализа (ДТГ) свидетельствуют о том, что первичная потеря массы от 8 до 15 мас.% в образце может быть связана с испарением адгезионной воды при температуре ниже 350°C, а также дегидратацией структурных вода в более высоких температурных диапазонах. Рентгенограммы сырой керамической пасты указывают на присутствие глинистых минералов, таких как монтмориллонит и мусковит, кварц и полевые шпаты. Процесс дегидроксилирования монтмориллонита характеризуется отчетливыми пиками на кривых ДТА, что позволяет понять происходящие структурные изменения. Исследованы ТЛ-свойства кварца, включая ТЛ-эмиссию и зависимость от дозы, что позволяет оценить дозу насыщения на уровне 13,2 кГр.

Ключевые слова: монтмориллонит, кальцит, глина, термогравиметрия, термолюминесценция, радиоактивные отходы.

RADİOAKTİV TULLANTILARIN BƏRK HALA GƏTİRİLMƏSİ ÜÇÜN KERAMİKA PASTASINDAN İSTİFADƏ EDİLMƏSİNİN TƏDQİQİ

S.Q. Məmmədov, M.Ə. Qurbanov, A.Z. Abışov, A.S. Əhədova, A.B. Əhədov

Xülasə: Bu məqalədə radioaktiv maddələri bərk hala salmaq üçün radioaktiv betondan hazırlanmış məhlullarda alternativ kimi istifadə oluna bilən xam keramika pastasının termoqravimetrik (TQ), termolüminesans (TL) və rentgen difraksiya (XRD) tədqiqatları təqdim olunur. TQ və diferensial termiki analizin (DTG) nəticələri göstərir ki, nümunədə ilkin kütlə itkisi 8-dən 15 %-ə qədər təşkil edir. Bu itki, 350°C-dən aşağı temperaturda adsorbsiya olunmuş suyun buxarlanması, daha yüksək temperatur diapazonlarında isə struktur suyunun dehidrasiyası ilə əlaqələndirilə bilər. Xam keramika pastasının rentgen difraksiya nümunələri montmorillonit və muskovit, kvars və feldispat kimi gil minerallarının mövcudluğunu göstərir. Montmorillonitin dehidroksilləşmə prosesi DTA əyrilərində xüsusi piklərlə xarakterizə olunur ki, bu da bizə baş verən struktur dəyişikliklərini başa düşməyə imkan verir. Kvarsın TL xassələri, o cümlədən TL emissiyası və TL intensivliyinin dozadan asılılığı öyrənilmişdir ki, bu da bizə doyma dozasını 13,2 kGy-də qiymətləndirməyə imkan verir.

Açar sözlər: montmorillonit, kalsit, gil, termoqravimetriya, termolüminesans, radioaktiv tullantılar.